fore, the absorption of radiation by inert particles is found to play an important role in indirectly igniting combustible gases.

The change of particle number density at a fixed particle size also exerted a strong influence such that the smaller the particle number density, the longer the ignition delay. As the particle number density decreases, the radiation plays a smaller role, because the absorption coefficient decreases with a fixed particle size and the ignition delay increased.

Acknowledgments

Financial assistance from the Objective Research Fund of the Korea Science and Engineering Foundation is gratefully acknowledged. The author is also indebted to T. F. Smith, the Associate Editor, for his efforts in improving this manuscript.

References

[1]Smith, T. F., Byun, K. H., and Chen, L. D., "Effects of Radiative and Conductive Transfer on Thermal Ignition," *Combustion and Flame*, Vol. 73, No. 1, 1988, pp. 67–74.

[2]Baek, S. W., "Ignition of Particle in Slab Geometry," *Combustion and Flame*, Vol. 81, Nos. 3–4, 1990, pp. 366–377.

[3]Baek, S. W., "Ignition of Combustible Gases by Radiative Heating of Inert Particles," *Combustion and Flame*, Vol. 97, Nos. 3–4, 1994, pp. 418–422.

[4]Djavdan, E., Darabiha, N., Giovangigli, V., and Candel, S. M., "Strained Propane-Air Flames with Detailed and Reduced Kinetic Schemes," *Combustion Science and Technology*, Vol. 76, Nos. 3–4, 1991, pp. 287–309.

[5]Kee, R. J., Miller, J. A., and Jefferson, T. H., "CHEMKIN: A General-Purpose, Problem-Independent, Transportable, Fortran Chemical Kinetics Code Package," Sandia Rept. 80-8003, 1980.

[6]Brewster, M. Q., "Radiation-Stagnation Flow Model Aluminized Solid Rocket Motor Internal Insulator Heat Transfer," *Journal of Thermophysics and Heat Transfer*, Vol. 3, No. 2, 1989, pp. 132–139.

Effective Stagnant Thermal Conductivity of Wire Screens

C. T. Hsu,* K. W. Wong,† and P. Cheng‡
Hong Kong University of Science and Technology, Clear Water Bay, Kowloon, Hong Kong

Nomenclature

A	= parameter of the wire screen in Eq. (1), d/w
a	= length of the cross-sectional area of the bars in the x direction
B	= parameter of the wire screen in Eq. (1), d/t
b	= length of the cross-sectional area of the bars in the z direction
c	= length of one side of the contact area
d	= diameter of the wire
k_{ex}, k_{ey}, k_{ez}	= effective thermal conductivities of the wire screens in the three principal directions
k_f	= thermal conductivity of the fluid phase
k_s	= thermal conductivity of the solid phase
l_x, l_y, l_z	= spacing of wires in the x, y, and z directions, respectively
t	= thickness of a layer of screen in Eq. (1)
w	= opening of wires in Eq. (1)
α	= empirical constant in Eq. (1)
$\gamma_{ax}, \gamma_{ay}, \gamma_{bz}$	= a/l_x, a/l_y, and b/l_z, respectively
γ_c	= c/a
λ	= fluid/solid conductivity ratio

Received March 27, 1995; revision received Nov. 14, 1995; accepted for publication Nov. 20, 1995.

*Senior Lecturer, Department of Mechanical Engineering. Member AIAA.

†Research Assistant, Department of Mechanical Engineering. Member AIAA.

‡Professor and Head, Department of Mechanical Engineering. Senior Member AIAA.

I. Introduction

An accurate prediction of the effective thermal conductivity of wire screens saturated with fluids is needed for the design of heat pipes[1] and the regenerators of Stirling machines. Although Maxwell's analytical expression[2] for the thermal conductivity of a porous medium has been widely used for the design of fluid-saturated screen wicks in heat pipes,[1] it is known that this expression is inaccurate in comparison with experimental data. Alexander[3] obtained an empirical correlation equation for thermal conductivities of sintered layers of wire screens saturated with water and air. Van Sant and Malet[4] carried out an experiment to measure effective thermal conductivities of 100-mesh size of stainless steel screens and copper screens saturated with water, CH_3OH, CCl_3F, and air, respectively. Comparing Van Sant and Malet's[4] data with Maxwell's expression[2] and Alexander's correlation,[3] Chang[5] found that the former underpredicts the effective thermal conductivity at large solid/fluid thermal conductivity ratios, whereas the latter overpredicts the effective thermal conductivity substantially. Using an electric analogy, Chang[5] obtained the following algebraic expression for the effective thermal conductivity of wire screens in the direction perpendicular to the layers of wires

$$\frac{k_{ez}}{k_f} = \frac{1}{(1+A)^2}\left(\alpha^2 A\left\{\frac{\alpha A}{\alpha - \pi B(1-\lambda)/2} + \frac{2[1 + A(1-\alpha)]}{\alpha - \pi B(1-\lambda)/4}\right\} + [1 + A(1-\alpha)^2]\right) \tag{1}$$

In matching Eq. (1) with Van Sant and Malet's experimental data,[4] Chang[5] found that the value of α is approximately equal to unity. In this Note, we idealize the screens as alternate layers of parallel solid bars, and apply the lumped parameter method[6] to obtain algebraic expressions for the effective thermal conductivity of screens in three principal directions. The major difference between Chang's model[5] and the present model is that contact resistance between the wires will be taken into consideration in the present work. For the specific case of alternate layers of parallel and perpendicular bars of equal spacing, the predicted thermal conductivity in the direction perpendicular to the layers of screen is found in reasonably good agreement with Van Sant and Malet's experimental data.[4] In addition, we have obtained algebraic expressions for the thermal conductivity of wire screens in the direction parallel to the layers of wire screens that has not been considered previously.

II. Application of the Lumped Parameter Method

We now idealize a stack of wire screens as layers of parallel and perpendicular bars of rectangular cross sections laid on the x–y plane as shown in Fig. 1a. It is noted that the undulation effect of wires weaving into screens is neglected through this idealization. The bars parallel in the x direction are separated by a distance of l_y, having a rectangular cross section of $(a \times b)$ (see Fig. 1b). On the other hand, the bars parallel in the y direction are separated by a distance of l_x, having a cross section of $(a \times b)$. If the wire screens consist of circular wires of d, the circular wires will be approximated as square bars with an equivalent area $a \times a$, while the contact areas between the wires in the z direction will be approximated by small rectangular blocks with a square cross-sectional area of $c \times c$ (see Fig. 1). The length c of the contact area between two consecutive layers of screens is a parameter whose value depends on the loading stress during the packing of the

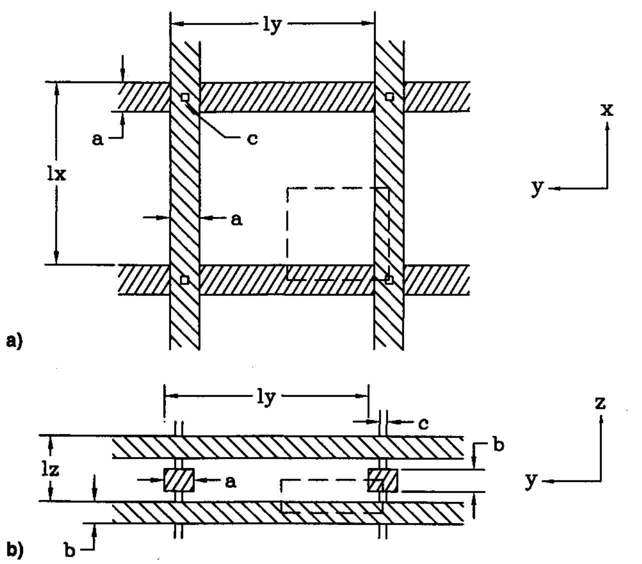

Fig. 1 a) Top and b) side views of wire screens and its unit cell (indicated by dashed lines).

screens. Note that l_x, l_y, and l_z are independent geometric parameters that are determined by how the wires are woven to form the screens. If the values of l_x, l_y, and l_z are different, the effective thermal conductivities of the wire screens in the three principal directions (k_{ex}, k_{ey}, and k_{ez}) will be different. To obtain algebraic expressions for the effective stagnant thermal conductivity of the wire screens in these three principal directions based on the lumped parameter method,[6] a unit cell of the size of ($l_x/2$, $l_y/2$, and $l_z/2$) containing one-eighth of the periodic structure of the wire is selected. This unit cell, as viewed from the z and x axes, is shown as dashed lines in Figs. 1a and 1b.

A. Effective Thermal Conductivities k_{ex} and k_{ey}

Consider first the effective thermal conductivity of the screens in the x direction. The unit cell viewed from the x axis is shown in Fig. 1b, which is composed of four layers in parallel: a fluid layer, a solid layer, and two composite layers. Here, the heat flux is assumed to be in the x direction. Based on the lumped parameter method,[6] the effective stagnant thermal conductivity of the wire screens in the x direction is therefore given by

$$\frac{k_{ex}}{k_f} = [1 - \gamma_{ay}\gamma_{bz} - \gamma_{bz} - \gamma_{ay}\gamma_c(1 - 2\gamma_{bz})] + \frac{\gamma_{ay}\gamma_{bz}}{\lambda} + \frac{\gamma_{bz}}{\gamma_{ax}(\lambda - 1) + 1} + \frac{\gamma_{ay}\gamma_c(1 - 2\gamma_{bz})}{\gamma_{ax}\gamma_c(\lambda - 1) + 1} \tag{2}$$

The expression for k_{ey} in the y direction can be obtained by interchanging between γ_{ax} and γ_{ay} in Eq. (2).

B. Effective Thermal Conductivity k_{ez}

To compute the effective thermal conductivity in the z direction, the unit cell as viewed from the z axis consists of four parallel columns (see Fig. 1a): a fluid layer, a solid layer, and two composite layers. Based on the lumped parameter model,[6] the effective stagnant thermal conductivity of wire screens in the z direction is

$$\frac{k_{ez}}{k_f} = (1 - \gamma_{ay})(1 - \gamma_{ax}) + \frac{(\gamma_{ax} + \gamma_{ay} - 2\gamma_{ax}\gamma_{ay})}{\gamma_{bz}(\lambda - 1) + 1} + \frac{\gamma_{ax}\gamma_{ay}(1 - \gamma_c^2)}{2\gamma_{bz}(\lambda - 1) + 1} + \frac{\gamma_c^2\gamma_{ax}\gamma_{ay}}{\lambda} \tag{3}$$

Eq. (3) with $\gamma_c = 0$ and $\gamma_{ay} = \gamma_{ax}$ reduces to Eq. (1) if we note that $A = d/w = \gamma_{ax}/(1 - \gamma_{ax})$ and let $B = 4\gamma_{bz}/\pi$, and $\alpha = 1$ in Eq. (1). Thus, the present model is more general than Chang's model.[5]

III. Results and Discussion

Equations (2) and (3) show that the effective thermal conductivities of wire screens depend on the parameters γ_{ax}, γ_{ay}, γ_{bz}, γ_c, and λ. Since $a \leq l_x$, $a \leq l_y$, $b \leq l_z$, and $c \leq a$, therefore, $\gamma_{ax} \leq 1$, $\gamma_{ay} \leq 1$, $\gamma_{bz} \leq 1$, and $\gamma_c \leq 1$. These values are zero if the bars are not touching each other, whereas these values become unity if the bars are touching each other. To compare with Van Sant and Malet's experimental data,[4] the evaluations of Eqs. (2) and (3) were carried out based on the following simplifications:

1) The periodic distance in the z direction l_z is equal to twice the diameter of the circular wires, i.e., $l_z = 2d$.

2) The deformation of the cross section of the circular wires during weaving is negligible, i.e., $a = b$.

3) The circular wires can be approximated by square bars with the same cross-sectional area, i.e., $a = b = \sqrt{\pi}d/2$.

4) $\gamma_c = 0.1$, the contact area between wires is $\gamma_c^2 = 0.01$.

Under the assumptions 1–3, we have $\gamma_{bz} = \sqrt{\pi}/4$. Computations of the effective thermal conductivities as functions of λ were carried out for various values of γ_{ax} and γ_{ay}. Because k_{ey} can be obtained by exchanging γ_{ax} and γ_{ay} in the expression for k_{ex}, it suffices to present only the results for k_{ex}.

A. Calculated Results of k_{ex}/k_f

It is important to note that in the evaluation of k_{ex}, the value of γ_{ay} is a measure of the relative importance of the layers-in-parallel effect of the solid phase, whereas the value of γ_{ax} is a measure of the layers-in-series effect of the solid phase. This is also reflected in Eq. (2) where k_{ex}/k_f is linearly proportional to γ_{ay} while inversely proportional to γ_{ax}. Figures 2a–2c show the effects of the spacing between solid bars on k_{ex}/k_f for various thermal conductivity ratios k_s/k_f. They demonstrate how the layers-in-series effect and the layers-in-parallel effect compete with each other when these spacing parameters change. Figure 2a shows the six curves of $\gamma_{ay} = 0$, 0.2, 0.4, 0.6, 0.8, and 1.0 with γ_{ax} being fixed at 0.5. Note that for the case of $\gamma_{ay} = 0$ and $\gamma_{ax} = 0.5$, the medium consists of fluid phase and solid bars perpendicular to the heat flow direction; consequently, the variations of k_{ex}/k_f is not a horizontal line. Note also this case ($\gamma_{ay} = 0$ and $\gamma_{ax} = 0.5$) behaves quite similarly to the results of a two-dimensional nontouching cylinders model with layers-in-series characteristics.[6] For $\gamma_{ay} > 0$, the layers-in-parallel effect becomes dominant over the layer-in-series effect at large k_s/k_f. In general, the behavior of the effective thermal conductivity in this case is similar to the phase symmetric model.[7]

Figure 2b shows the effect of varying γ_{ax} on k_{ex}/k_f of a stack of screens composed of parallel and perpendicular bars at a fixed value of $\gamma_{ay} = 0.5$. Here, the six curves correspond to $\gamma_{ax} = 0$, 0.2, 0.4, 0.6, 0.8, and 1.0. With γ_{ay} being fixed, the variation in γ_{ax} shows the layers-in-series effect on the effective thermal conductivity. The curves become linear when k_s/k_f becomes large. This is because when k_s/k_f becomes large, heat transfer is dominated by conduction through solid bars parallel to the heat flux direction, and $k_{ex}/k_f \to (\gamma_{bz}\gamma_{ay})(k_s/k_f) = 0.222(k_s/k_f)$ when $\gamma_{ax} \neq 1$. When $\gamma_{ax} = 1.0$, $\gamma_{bz}(1 + \gamma_{ay})$ of the unit cell becomes a solid column in parallel to heat flux direction and $k_{ex}/k_f \to 0.665(k_s/k_f)$. Note that there is a jump in the value of k_{ex}/k_f when $\gamma_{ax} = 1$. Except for this jump case of $\gamma_{ax} = 1$, it is clear from Fig. 2b that the effect of varying γ_{ax} (bars-in-series process) is confined in the range of $1 \leq k_s/k_f \leq 10^2$ and is not significant. Figure 2c shows the effective thermal conductivity k_{ex} of screens composed of equal spacing parallel and perpendicular bars (i.e., $\gamma_{ax} = \gamma_{ay}$). The special case of $\gamma_{ax} = \gamma_{ay} = 0$ in Fig. 2c corresponds to a medium consisting of the fluid phase only, and therefore, $k_{ex}/k_f = 1$ is a horizontal line. Since the geometry of this figure is very similar to that in Fig. 2a, the behavior of the effective thermal conductivity is qualitatively similar to each other. By setting $\gamma_{ax} = \gamma_{ay}$, it is clear that the layers-in-parallel effect plays the dominant role over the layers-in-series effect in determining the effective thermal con-

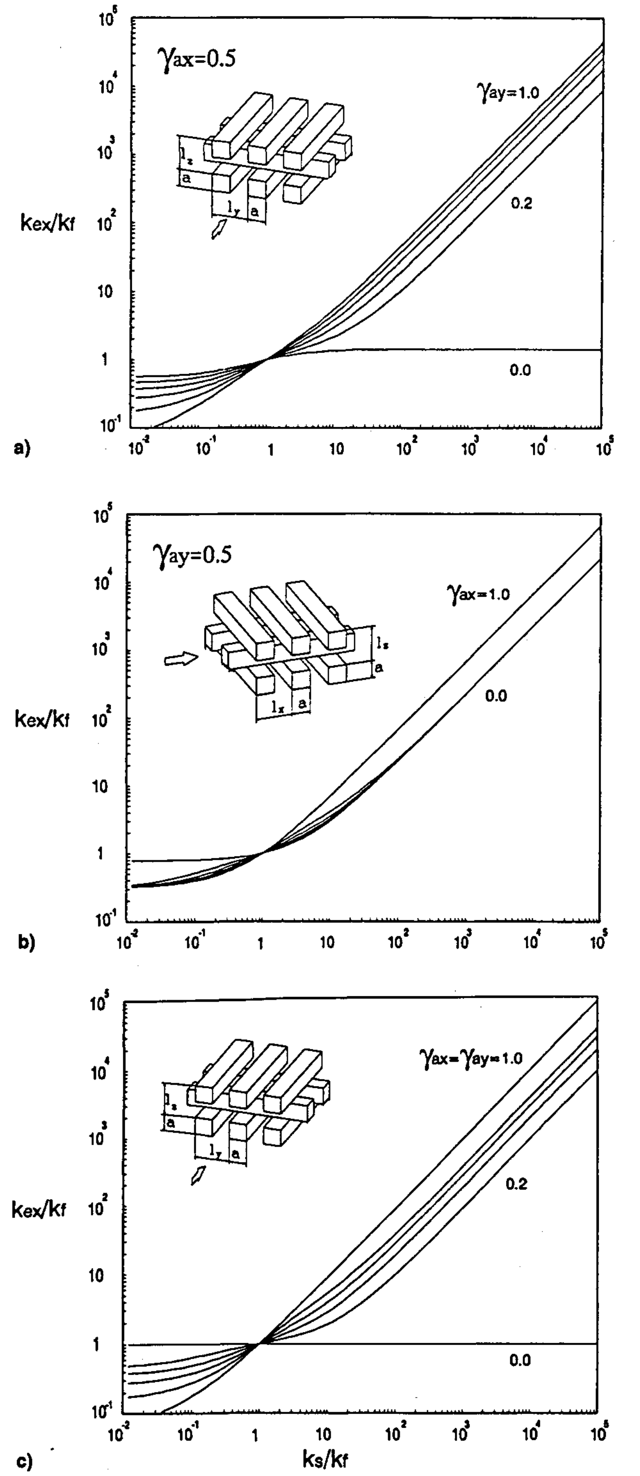

Fig. 2 Effects of bar spacing on k_{ex}/k_f for $\gamma_{bz} = \sqrt{\pi}/4$ and γ_c = 0.1: a) bars-in-parallel effects, b) bars-in-series effects, and c) $\gamma_{ax} = \gamma_{ay}$.

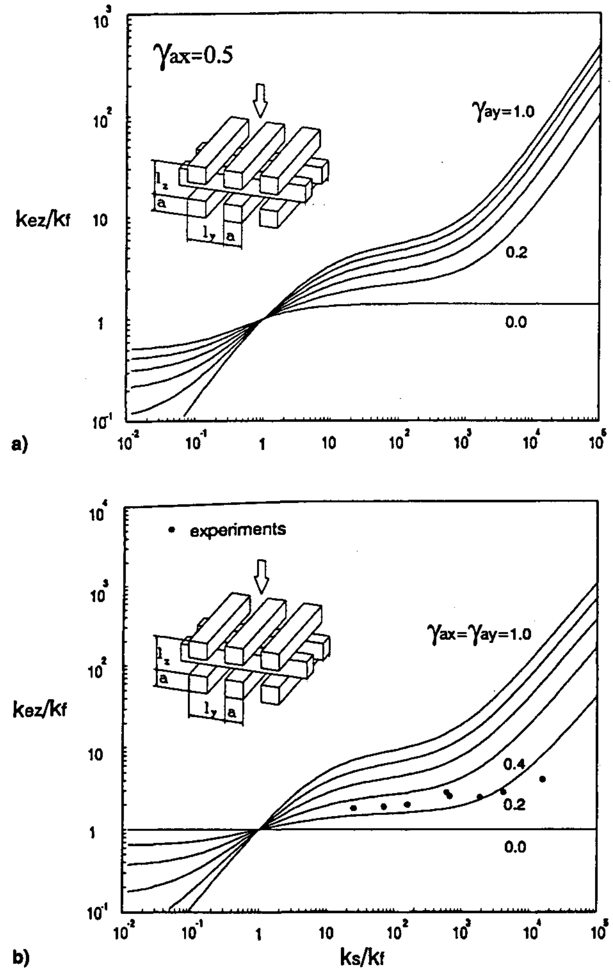

Fig. 3 Effects of bar spacing on k_{ez}/k_f for $\gamma_{bz} = \sqrt{\pi}/4$ and γ_c = 0.1: a) γ_{ax} = 0.5 with various values of γ_{ay} and b) $\gamma_{ax} = \gamma_{ay}$.

ductivity. Again, the behavior is quite similar to the phase symmetry model.[7] Under the condition of $\gamma_{ax} = \gamma_{ay}$, the thermal conductivities in the x and y directions are equal, i.e., $k_{ex} = k_{ey}$.

B. Calculated Results of k_{ez}/k_f

Figure 3a shows the effect of the solid bar spacing perpendicular to the direction of heat flux on the effective thermal conductivity in the z direction k_{ez}/k_f. It shows the effect of varying γ_{ay} on k_{ez}/k_f when γ_{ax} is fixed at 0.5. The case of γ_{ay} = 0 corresponds to an array of nontouching bars perpendicular to the direction of heat flux. For $\gamma_{ay} \neq 0$, the results shown in Fig. 3a are quite similar to those of a three-dimensional cubes model studied earlier.[6] In the range of $1 < k_s/k_f < 10^3$, the effective thermal conductivity k_{ez}/k_f is dominated by the layers-in-series mechanism, whereas for $k_s/k_f > 10^3$, the thermal resistance because of touching becomes dominant. The case of γ_{ay} = 1 corresponds to a stack of screens composed of perpendicular touching bars. Figure 3b shows the results of k_{ez}/k_f calculated from Eq. (3) for equal spacing bars with $\gamma_{ax} = \gamma_{ay}$ varying from 0 to 1.0. For comparison purposes, Van Sant and Malet's eight experimental data points[6] with porosity corresponding to γ_{ax} = 0.34–0.41 are also presented in the same graph. It is shown that the calculated results based on Eq. (3) with $\gamma_c = 0.1$, $\gamma_{bz} = \sqrt{\pi}/4$, and $\gamma_{ax} = \gamma_{ay} = 0.3$ are in reasonably good agreement with experimental results.[6]

IV. Concluding Remarks

In this Note, algebraic expressions for the thermal conductivities of wire screens are obtained based on the lumped parameter method. The stack of wire screens is modeled as alternative layers of parallel solid bars aligned perpendicularly to each other. The three-dimensional unit cell consists of two layers of parallel bars perpendicular to each other with four independent spacing parameters γ_{ax}, γ_{ay}, γ_{bz}, and γ_c. A comparison of the predicted thermal conductivity of wire screens (in the direction perpendicular to the wires) based on the present model with existing data shows that they are in reasonably good agreement.

Acknowledgments

This work was supported by the Chiang Industrial Charity Foundation under a Research Award RH92104 and by the Hong Kong RGC Earmarked Research Grant HKUST575/94E.

References

[1]Chi, S. W., *Heat Pipe Theory and Practice*, McGraw-Hill, New York, 1976, pp. 213–226.

[2]Maxwell, J. C., "A Treatise on Electricity and Magnetism," Vol. 1, 3rd ed., Oxford Univ. Press, Oxford, England, UK, 1954.

[3]Alexander, E. G., Jr., "Structure-Property Relationships in Heat Pipe Wicking Materials," Ph.D. Dissertation, Dept. of Chemical Engineering, North Carolina State Univ., Raleigh, NC, 1972.

[4]Van Sant, J. H., and Malet, J. R., "Thermal Conductivity of Some Heat Pipe Wicks," *Letters in Heat and Mass Transfer*, Vol. 2, 1975, pp. 199–206.

[5]Chang, W. S., "Porosity and Effective Thermal Conductivity of Wire Screens," *Journal of Heat Transfer*, Vol. 112, No. 5, 1990, pp. 5–9.

[6]Hsu, C. T., Cheng, P., and Wong, K. W., "A Lumped Parameter Model for Stagnant Thermal Conductivity of Spatially Periodic Porous Media," *Journal of Heat Transfer*, Vol. 117, 1995, pp. 264–269.

[7]Hsu, C. T., Cheng, P., and Wong, K. W., "Modified Zehner-Schlunder Models for Stagnant Thermal Conductivity of Porous Medium," *International Journal of Heat and Mass Transfer*, Vol. 37, No. 17, 1994, pp. 2751–2759.

New Chill-Block Melt Spinning Relations to Predict Ribbon Thickness

David J. Kukulka*
State University of New York at Buffalo, Buffalo, New York 14222
Anant Poopisut†
M. W. Kellogg Company, Houston, Texas 77072
and
Joseph C. Mollendorf‡
State University of New York at Buffalo, Buffalo, New York 14260

Nomenclature

A, B, C_b, K	=	equation constant
l	=	liquid puddle length
Q	=	volumetric flow rate
Q_{jet}	=	volumetric jet flow
t	=	ribbon thickness
U_∞	=	liquid velocity
V	=	substrate velocity
w	=	ribbon width
α	=	ejection angle, measured from vertical axis
δl	=	boundary-layer displacement thickness
ν	=	kinematic viscosity

Introduction

Amorphous metallic alloys, sometimes called glassy alloys, are useful materials that have attractive properties that include good corrosion resistance and high fracture strength. Methods that are utilized in producing amorphous metals include vapor condensation, sputtering, ion implantation, and chill-block melt spinning. Chill-block melt spinning is a relatively simple process whose origin dates back into the 1800s. It is widely used in the mass production of a variety of products (i.e., amorphous superalloy brazing alloys, solders, glassy transformer core alloys, and other ferromagnetic products). Pond[1] patented a process that involved ejecting a jet of liquid metal onto the surface of a rotating drum. In chill-block spinning, the material is melted in a crucible and a stream of melt is ejected by pressure through a small orifice onto the circumferential surface of a rotating drum. A liquid puddle forms at the base of the jet and the ribbon is extracted from its underside. Kavesh[2] analyzed the melt puddle in a chill-block melt spinning process by assuming that the viscosity of the liquid outside the solidified layer is constant and that no thermal resistance exists at the liquid melt/substrate interface. He showed that the thermal boundary-layer thickness was three to nine times thicker than the momentum thickness. Hillmann and Hilzinger[3] studied $Fe_{40}Ni_{40}P_{14}B_6$ and found that at a constant ejection pressure the height of the puddle was of secondary importance and that the dimensions of the ribbon could be determined by the length and width of the puddle. Liebermann[4] developed an experimental relation and found no significant effect of melt superheat on the geometry of ribbons produced from $Fe_{40}Ni_{40}B_{20}$ and $Fe_{83}B_{15}Si_2$. Vincent et al.[5] calculated the rate of the propagation of the solid front by assuming a heat transfer coefficient and found that the solid front velocity was too low to account for the final ribbon thickness. They concluded that the solid ribbon thickness is related primarily to the propagation of the momentum. Vincent et al. presents a discussion supporting momentum control as being dominant in the chill-block melt spinning process.

Pavuna[6] experimentally studied chill-block melt spinning over a wide range of volumetric flow rates for a melt with an approximate dynamic viscosity of 965 mm^2/s. For flow rates up to 4 cm^3/s Liebermann's[4] relation is supported, whereas for higher flow rates (from 4 to 7 cm^3/s) the data agree with the relations of Kavesh.[2] Pavuna[6] concludes that ribbon width is primarily controlled by the normal component of the volumetric flow rate and that the injection angle may influence both ribbon width and thickness.

Anestiev and Russeo[7] proposed a relationship between the puddle length, volumetric flow rate, surface velocity, impingement angle, and nozzle diameter. Anestiev[8] presented a system of equations that uses casting parameters and several physical properties of the melt to predict ribbon thickness. These results show good agreement with experimental data, but require the use of a series of equations to obtain results. In a later study, Anestiev[9] considered the existence of a heat transfer resistance on the puddle-substrate contact area and the latent heat of fusion separation on the liquid–solid interface. Finally, Taha et al.[10] graphically investigated the variation of ribbon geometry as a function of substrate velocity, injection pressure, substrate thermal conductivity, melt superheat, nozzle/substrate height, and nozzle diameter.

Proposed Relations

The present study proposes two empirical relations that predict ribbon thickness for a wide range of volumetric flow rates (where $Q = Vwt$). The first relation is based on experimental data, whereas the second uses a momentum transport control analysis. Since ribbon formation is complex in nature, it is difficult for a simple relation to describe a wide range of conditions. Based on the form of previous works, the general form of the proposed relations can be taken as

$$t \sim Q^A/V^B \tag{1}$$

$$w \sim Q^{1-A}/V^{1-B} \tag{2}$$

Pavuna[6] reported that both Kavesh's[2] and Liebermann's[4] relations could not describe the entire range of his experimental

Received May 15, 1995; revision received March 25, 1996; accepted for publication March 25, 1996.

*Professor, Department of Mechanical Engineering Technology, 1300 Elmwood Avenue.

†Research Engineer.

‡Professor, Department of Mechanical and Aerospace Engineering.